Formation of epitaxial β-FeSi$_2$ films on Si(001) as studied by medium-energy ion scattering

K. Konuma, J. Vrijmoeth, P. M. Zagwijn, J. W. M. Frenken, E. Vlieg, and J. F. van der Veen

Formation of epitaxial β-FeSi$_2$ films on Si(001) as studied by medium-energy ion scattering

K. Konuma,[a] J. Vrijmoeth,[b] P. M. Zagwijn, J. W. M. Frenken, E. Vlieg, and J. F. van der Veen

FOM-Institute for Atomic and Molecular Physics, Kruislaan 407, 1098 SJ Amsterdam, The Netherlands

Ultrathin (~ 1.3 nm) epitaxial films of β-FeSi$_2$ were grown on Si(001) by room temperature (RT) deposition of Fe followed by annealing. During the various stages of the growth process, the lattice structure, composition, and morphology of the films were investigated by medium-energy ion scattering in conjunction with shadowing and blocking. At RT, the deposited Fe reacts with the Si(001) substrate and forms a continuous film of average composition FeSi. After annealing to 670 K, a conversion into β-FeSi$_2$ has taken place and the film is no longer continuous. Further annealing at higher temperatures results in the formation of islands of increasing height. The β-FeSi$_2$ films grown are composites of two azimuthal orientations with respect to the substrate: The predominant A orientation with β-FeSi$_2$ [010]|| Si⟨110⟩ and the B orientation with β-FeSi$_2$ [010] || Si⟨100⟩. The lattice strain in the films is partially relaxed. At the interface, the Fe atoms are found to be displaced from bulk lattice sites. These displacements are thought to be associated with the formation of atomic bonds at the interface of the dissimilar β-FeSi$_2$(100) and Si(001) lattices.

I. INTRODUCTION

The controlled formation of thin epitaxial silicide films on Si(001) substrates is of great importance for various applications in Si large-scale integration LSI technology. One of the silicides, FeSi$_2$, exists in two phases, the metallic α phase and the semiconducting β phase. The narrow and direct band gap of 0.87 eV of β-FeSi$_2$ makes this phase a promising candidate for use in infrared detectors and light-emitting devices.[1] A requirement for integration in Si technology is that large-area continuous epitaxial films of the β phase can be grown over a sufficiently large temperature interval.

β-FeSi$_2$ has an orthorombic Bravais lattice with lattice parameters $a = 9.863$, $b = 7.791$, and $c = 7.833$ Å.[2] The formation of epitaxial β-FeSi$_2$ films on Si(001) has been reported previously.[3-5] The β-FeSi$_2$ growth face is the "a-face" or the (100) plane.[6] Growth is performed by either molecular beam epitaxy (MBE), reactive deposition epitaxy (RDE), or solid phase epitaxy (SPE). It appears that control over the epitaxy of thick β-FeSi$_2$ films can be achieved by the use of ultrathin predeposited films that serve as templates for further growth.[7] β-FeSi$_2$ grows epitaxially on Si(001) in two different lattice-matching orientations, depending on growth method and temperature: The A-type orientation with β-FeSi$_2$ [010]|| Si⟨110⟩ or the B orientation with β-FeSi$_2$ [010]|| Si⟨100⟩.[6] The A orientation is the predominant one over a wide range of growth temperatures and it is the orientation commonly found. Note that for a given epitaxial relationship (A or B), there are still two azimuthal orientations possible that are crystallographically equivalent; for the A-type epitaxy these are the orientations β-FeSi$_2$[010]|| Si[110] and β-FeSi$_2$[001] || Si[110]. This double positioning finds its origin in the four-fold symmetry of the Si crystal around the [001] axis.

Other problems commonly encountered in the epitaxial growth of β-FeSi$_2$ films are a possible conversion of β-FeSi$_2$ into the metalic α-FeSi$_2$ phase at temperatures exceeding 1173 K,[8] variations in film thickness, and islanding at elevated temperatures. The stress induced by the lattice mismatch with Si(001) may be a driving force for islanding and for other types of defects in the film or at the interface. Many of the above issues have remained virtually unexplored.

Here we report a medium-energy ion scattering (MEIS) study of the formation of ultrathin (~ 1.3 nm) β-FeSi$_2$ films on Si(001). The films were grown by SPE. Deposition of Fe at room temperature (RT) was found to result in the formation of a FeSi phase, out of which the β-FeSi$_2$ phase grew upon heating. The β-FeSi$_2$ lattice structure and epitaxial orientation were identified by the combined use of shadowing and blocking. A depth resolution of 0.1 nm enabled us to investigate the interfacial abruptness and the film morphology after various heat treatments.

II. EXPERIMENT

The Fe deposition, the heat treatments, and the MEIS measurements were performed in an ultrahigh vacuum (UHV) analysis chamber (base pressure 7×10^{-9} Pa) coupled to a 200 kV ion accelerator.[9]

The Si(001) samples, with dimensions 16×6 mm^2, were cut from a P-doped wafer with a resistivity of 5–10 Ω cm. The miscut angle measured 0.11° toward the [110]

azimuthal direction. The samples were rinsed ultrasonically in high-purity ethanol and loaded into the vacuum system. The samples were cleaned by annealing to 1500 K for 3 min in a MBE apparatus connected to the analysis chamber. Then a Si buffer layer of 50 nm was deposited from an electron-beam evaporator at a substrate temperature of 950 K. The deposition rate was 0.13 nm/s. After this, reflection high-energy electron diffraction showed sharp 2×1 patterns.

Fe was evaporated by direct sublimation from a 99.99% pure Fe wire and deposited on the Si(001) surface at RT. The deposition rate was 1.2 ML/min and the total deposited amount of Fe was 5.0 ML. Here, one monolayer (1 ML) is defined as the number of atoms in a single Si(001) monolayer, which corresponds to 6.78×10^{14} atoms/cm^2. During deposition, the pressure did not exceed 7×10^{-8} Pa and quickly recovered afterwards. After Fe deposition, small amounts of C and O (<0.1 ML) were detected by Auger electron spectroscopy [the measured peak intensity ratios were O(KLL)/Si(LMM) = 0.03 and C(KLL)/Si(LMM) = 0.02]. MEIS was used to analyze the film after RT deposition and after heat treatments at 470 K for 15 min, 670 K for 10 min, 870 K for 2 min, and 1010 K for 30 s. The temperatures were set by direct-current heating of the sample and were read by an infrared pyrometer with an accuracy of 30 K.

The principles of MEIS and its application to thin-film analysis have been discussed elsewhere.[10] In brief, shadowing and blocking techniques are used to determine the crystal structure, the epitaxial orientation, and the lattice strain of the grown film. The film's composition and morphology are determined through analysis of the intensity and shape of the metal (Fe) and substrate (Si) peaks in the energy spectrum of backscattered ions.

The MEIS measurements were performed using 100 keV H$^+$ and He$^+$ beams collimated to within 0.1°. All data were collected in the ($\bar{1}$10) plane of the Si(001) substrate, with the incident beam aligned with the [11$\bar{1}$] channeling direction [Fig. 1(a)]. Backscattering ions were simultaneously detected over a 20° angular range using a toroidal electrostatic analyzer having an energy resolution of $\Delta E / E = 9 \times 10^{-4}$. In most measurements, the toroidal energy analyzer was centered around the [111] blocking direction, corresponding to an exit angle α of 35.26°. Exit angles in the range $8° < \alpha < 63°$ were covered by rotating the toroidal energy analyzer within the ($\bar{1}$10) scattering plane. The ultrahigh energy resolution of the electrostatic analyzer yields excellent depth resolution.[11] For the scattering geometry of Fig. 1(a) and assuming a stopping power of 670 or 760 eV/nm[12,13] depending on whether the film is FeSi$_2$ or FeSi, we estimate the resolution to be 0.1 nm.

Quantitative structure analyses of the epitaxial FeSi$_2$ films were performed by comparing the measured blocking patterns with patterns simulated for different structural models (α or β-FeSi$_2$) and epitaxial orientations (A or B). The simulations were performed by use of Monte Carlo techniques as discussed in Ref. 14. In the simulations we assume the Si and Fe atoms in the film to have root mean square (rms) thermal vibration amplitudes of 0.011 and
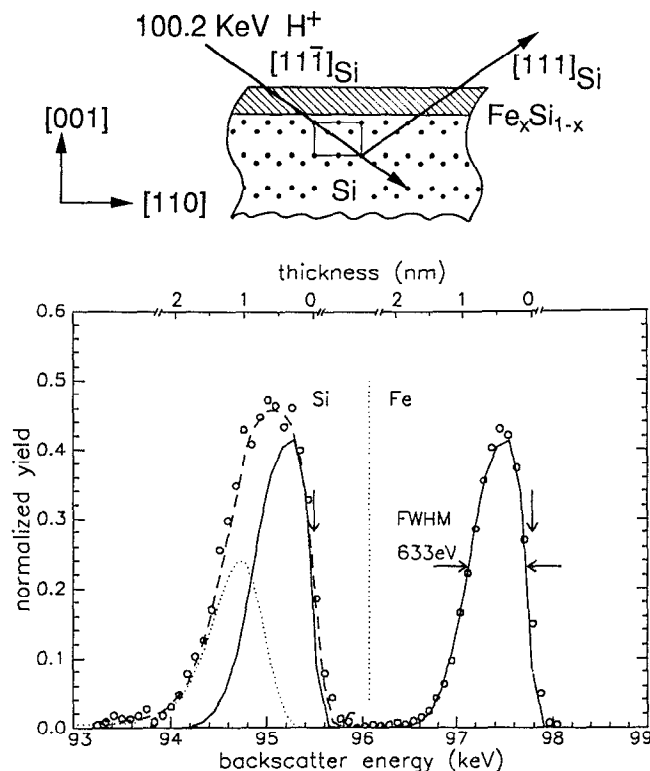

FIG. 1. (a) Scattering geometry used for the analyses of Fe-silicide films on Si(001). The scattering plane is the ($\bar{1}$10) plane of the Si substrate. The energy analyzer, which detects the backscattered ions over an angular range of 20°, is centered around the [111] blocking direction of the substrate. (b) Backscattering energy spectrum measured in the double alignment geometry shown in (a). The spectrum was taken from Si(001) with 5.0 monolayers of Fe deposited at room temperature. The arrows indicate the elastic surface backscattering energies for Fe and Si. The backscattering yields from Si and Fe have been normalized to the calculated random heights for the respective elements. The full curve through the measured Fe peak is the result of a fit assuming a continuous FeSi film. The solid curve through the Si peak is the fitted Fe curve shifted by the elastic energy difference between Si and Fe, while the dotted curve through the Si peak represents the backscattering contribution from the Si substrate. The dashed curve is the sum of the two contributions.

0.0095 nm, as for CoSi$_2$ and NiSi$_2$.[15,16] The rms vibration amplitude of the substrate Si atoms is taken to be 0.0078 nm.[17] All vibrations are assumed to be uncorrelated.

III. RESULTS

A. As-deposited film

The composition of the film after Fe deposition at RT was determined from the measured MEIS spectra. The spectrum shown in Fig. 1b was taken with a 100.2 keV H$^+$ beam. The selected detection direction was the [111] axis of the substrate. In the spectrum, the backscattering contributions from Si and Fe have been normalized to the calculated random heights of the respective elements. We find the normalized Si peak and the Fe peak to be approximately of the same height. Thus, the deposited Fe has reacted at RT with the Si substrate to form the monosilicide FeSi. The absence of a downward energy shift of the Si peak relative to the elastic backscattering energy is additional evidence that a reaction has occurred; burial of the
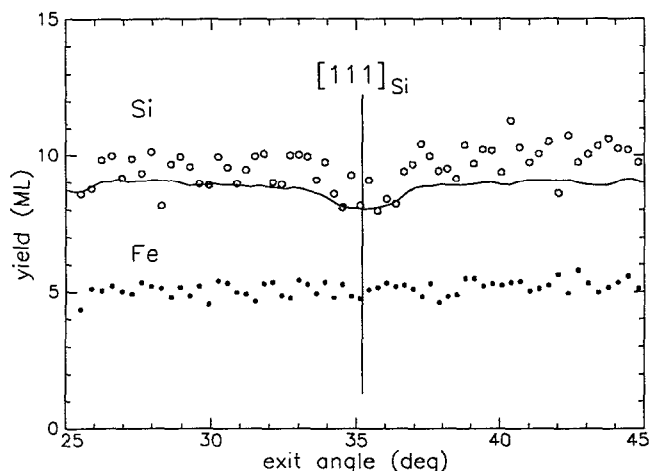
FIG. 2. Integrated areas of the Fe and Si backscattering peaks as a function of exit angle. The scattering geometry is that of Fig. 1(a). The measurements were performed on the RT deposited Fe on Si(001) system. The vertical line indicates the [111] blocking axis in the Si(001) substrate and the solid curve through the Si blocking pattern represents a Monte Carlo computer simulation for a bulk-like substrate plus 5.0 ML of randomly positioned Si atoms. The latter represents the reacted Si atoms in the FeSi film on top.
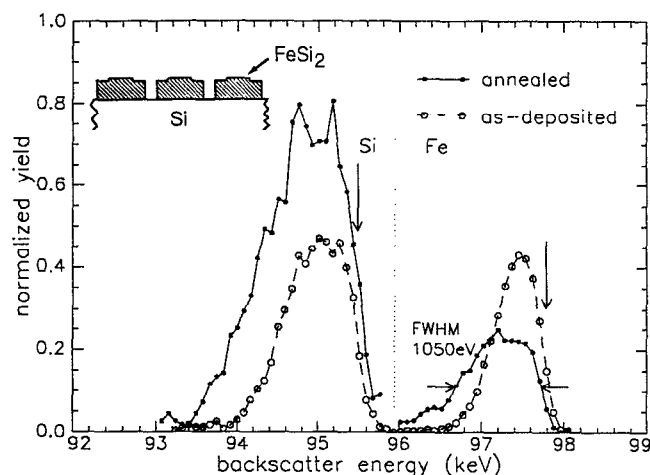
FIG. 3. Backscattering energy spectrum as in Fig. 1(b), but after annealing at 670 K (solid circles). For comparison the spectrum from the surface with FeSi film on top has been reproduced from Fig. 1(b) (open circles). After annealing, an islanded $FeSi_2$ film is obtained as indicated in the inset.

substrate by an unreacted Fe film would have resulted in a large shift by 312 eV.

The film's morphology (islanded or continuous) can be deduced from the peak widths. We find that the width of the Fe peak is about that expected for a continuous FeSi film formed out of the deposited amount of 5.0 ML. Using tabulated stopping cross sections for 100 keV H^+ in Si and Fe,[12] applying Bragg's rule[13] and taking the energy resolution of the system into account we estimate a width of 593 eV, which is close to the measured value of 633 eV (FWHM). Note that the Si peak is wider than the Fe peak, because it includes the backscattering contribution from the nonshadowed/nonblocked atoms in the top layers of the Si substrate. The data in Fig. 1(b) are inconsistent with pure Fe islands on top of unreacted Si because the total Si yield of ~9 ML in the surface peak is much larger than the ~3 ML expected for unreacted Si.

Next we consider the possible occurrence of epitaxy of the RT deposited film and the structural rearrangement at the interface. Figure 2 shows the blocking patterns derived from the Si and Fe backscattering yields over a 20° range of exit angles centered around the [111] substrate axis. Each point of the pattern represents the area of the Si (or Fe) peak at the corresponding exit angle, calibrated into the number of visible monolayers using the method described in Ref. 10. The absence of any blocking minimum in the Fe pattern shows that the FeSi film is either amorphous or polycrystalline, with random orientation of the crystallites. Hence, there is no epitaxy. However, a blocking minimum is seen in the Si pattern. The minimum, which occurs along the [111] direction, is evidently caused by blocking in the top layers of the Si(001) substrate lattice. The solid curve through the Si blocking pattern represents the sum of a Monte Carlo simulation for a bulk-like Si substrate and a constant yield of 5.0 ML. The latter contribution originates

from the randomly positioned Si atoms in the FeSi film. Apparently, the Si(001) surface, which in its clean state is reconstructed into dimer rows,[18] has reordered into a bulk-like structure in which the dimers have been "consumed" by the reacting Fe atoms.

The final step in our analysis of the RT reacted film is a fit of the complete energy spectrum to a model that features a homogeneous continuous FeSi film and an abrupt interface with a bulk-like Si substrate. The fitting procedure allows variations in the film thickness according to a gamma distribution[19] with the mean thickness and the variance as free parameters. Another free parameter in the fit is the number of visible substrate layers. The peak shapes and energy positions are calculated in the fit under the assumption of a random stopping cross section of 172 $eV/(10^{15}$ FeSi molecules/cm$^2)$ in FeSi and of 82 $eV/(10^{15}$ atoms/cm$^2)$ in Si.[12,13] The results of the fit is shown in Fig. 1(b), together with a decomposition of the Si peak into the best-fit contributions from the substrate and the film. The Si substrate peak area equals 2.9 ± 0.1 ML in good agreement with the number of 3.0 visible ML's calculated for a bulk-like lattice. The FeSi film is found to be 0.8 ± 0.05 nm thick.

B. Formation and thermal stability of β-FeSi$_2$

Heat treatment transforms the FeSi film into epitaxial $FeSi_2$. Figure 3 compares the spectrum from the as-deposited film [Fig. 1(b)] with one obtained in the same scattering geometry after heating at 470 K for 15 min followed by heating to 670 K for 10 min. The ratio of the Si to Fe peak heights is seen to increase, indicating the conversion of FeSi into $FeSi_2$. At the same time, the peaks broaden considerably, which reflects a thickening of the film as a result of the reaction with Si substrate atoms. The measured FWHM of the Fe peak (1050 eV) is 20% larger than is expected for a continuous $FeSi_2$ film. This indicates
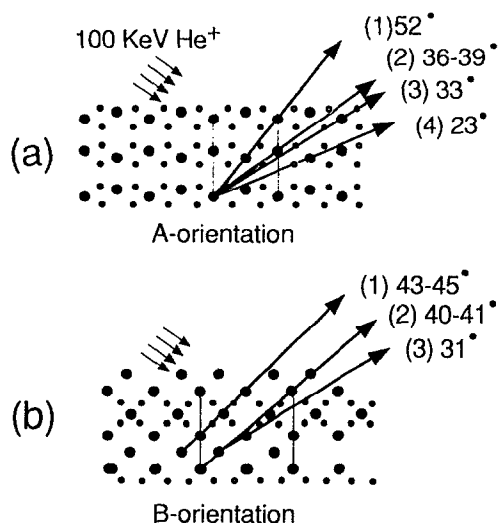
FIG. 4. The lattice structure for A and B oriented β-FeSi$_2$ projected onto the ($\bar{1}10$) scattering plane in the substrate (panels a and b, respectively). Closed and open circles denote Fe and Si atoms. For both orientations the main silicide blocking directions are indicated together with the corresponding exit angles.
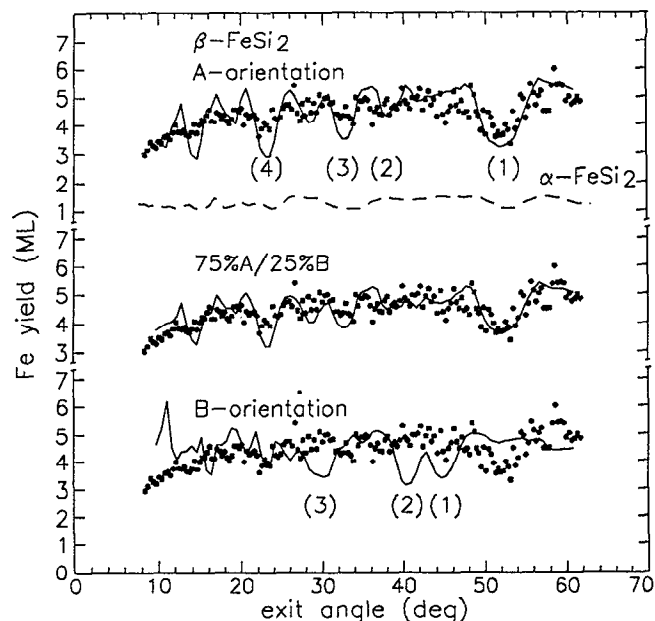

FIG. 5. Blocking patterns of the Fe yield after annealing the sample at 670 K. The scattering geometry is that of Fig. 4. Monte Carlo simulations are shown for β-FeSi$_2$ films that are (a) purely A oriented, (b) 75% A/25% B oriented, and (c) purely B oriented. Curve (b) yields the best fit to the data. The main blocking minima (1)–(4) are labeled as in Fig. 4 for the corresponding A and B orientations. For comparisons, a Monte Carlo simulation is shown for α-FeSi$_2$ (broken curve).

the formation of islands covering about 80% of the surface area. The Fe peak shape can be fit to a growth model that features mesa-shaped islands with heights in the range of 1.5–1.7 nm.

Next we determine whether the FeSi$_2$ lattice formed is of the β type with A or B orientation, or of the α type. To this end, we analyze blocking patterns of the Fe yield taken with 100 keV He$^+$ ions in the scattering geometry of Fig. 1(a).

First, we consider a β-type silicide. Figure 4 shows the lattice structure for the A and B orientations projected onto the ($\bar{1}10$) plane of the silicon substrate. The two orientations lead to distinctly different sets of blocking directions. The measured blocking pattern from Fe, shown in Fig. 5, has minima at angles that correspond exactly with the directions (1)–(4) in the A-oriented silicide. Indeed, Monte Carlo simulations for A-oriented β-FeSi$_2$ reproduce the measured pattern fairly well (top curve in Fig. 5). A better fit, however, is obtained for a 75%/25% mixture of A and B domains, each averaged over two equally probable 90° rotated orientations (middle curve). In the simulations, the silicide was assumed to be fully strained so as to match the substrate lattice and its thickness was assumed to be on average 6–7 atomic planes, corresponding to an average island thickness of 1.5–1.7 nm as derived from the Fe peak shapes. The interface structure was modeled as described in Sec. III C.

Second, we investigate the possibility that epitaxial α-type FeSi$_2$ is formed. The α-type FeSi$_2$ lattice is tetragonal with lattice parameters $a=b=2.695$ and $c=5.090$ Å. It is known to grow epitaxially on Si(001) with its main crystal axes aligned with the same directions in the substrate.[20] In our scattering geometry, this alignment would give rise to strong shadowing and blocking effects and therefore to backscattering yields much lower than we observe. A Monte Carlo simulation performed on lattice-

matched α-FeSi$_2$(001) (broken curves in Figs. 5 and 7) produces not only the wrong Fe yields but also blocking angles different from the ones measured. We conclude that the silicide is of the β phase.

We have also investigated the effect of additional heating on the morphology and structure of the film. Figure 6 shows energy spectra of the Fe backscattering peak measured after heating the substrate successively at 670 K for 10 min, 870 K for 2 min, and 1010 K for 30 s. The spectra
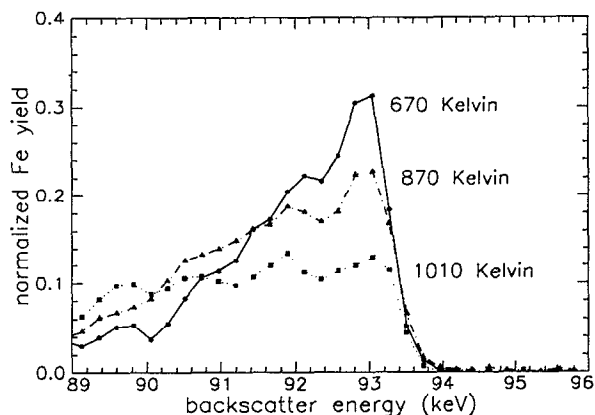

FIG. 6. Energy spectra of the Fe backscattering peak measured after heating the substrate successively at 670 K for 10 min, 870 K for 2 min, and 1010 K for 30 s. The spectra were taken with a He$^+$ ions incident along the [11$\bar{1}$] substrate direction and exiting at an angle of 22° with respect to the surface plane.
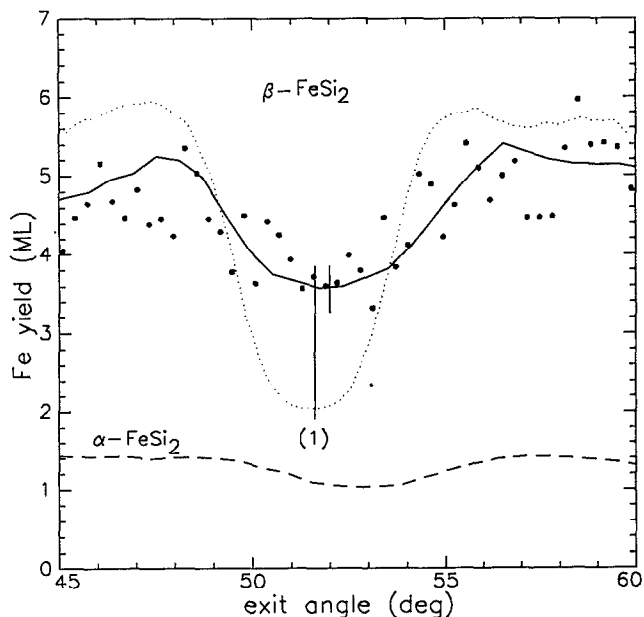
FIG. 7. Enlarged view of main blocking minimum in β-FeSi$_2$ around the exit angle of 52°. The dotted curve, with its minimum centered around the vertical line labeled (1), represents a simulation for a fully relaxed and 75% A/25% B-oriented β-FeSi$_2$ film with bulk structure up to the very interface, whereas the solid curve represents the best fit for the 75% A/25% B model with displaced Fe at the interface. The tickmark at the center of the measured blocking minimum is shifted upward by ~0.4° with respect to minimum (1), which indicates a partially relaxed compressive strain in the epitaxial film. The broken curve shows for comparison a simulation for α-FeSi$_2$.

were taken with the He$^+$ ions incident along the [11$\bar{1}$] substrate direction and exiting at an angle of 22° with respect to the surface plane. From the dramatic broadening of the peak, it is evident that the film breaks up in islands of increasing thickness. After annealing at 1010 K, the average thickness is 4 nm, which is 3.1 times the thickness expected for a continuous film. The lattice structure, however, remains β type, as is evident from the blocking patterns (not shown).

C. Lattice strain and atomic displacements at the interface

We now address the issue of whether the epitaxial β-FeSi$_2$ islands are laterally strained or relaxed. For the predominant A orientation, the lattice mismatch with the substrate is 1.4% along the FeSi$_2$[010] direction and 1.9% along the FeSi$_2$[001] direction. In the scattering plane, which runs parallel to the [010] or [001] direction in FeSi$_2$, lattice matching is therefore achieved for a lateral compression by 1.4% or 1.9%, respectively. The compression, which is accompanied by an expansion along the surface normal, tilts the blocking axes upward with respect to the ones in fully relaxed bulk silicide.[14] Assuming a ratio of perpendicular to parallel strain of 0.9 [21] we expect blocking minimum (1) to be tilted by about 0.9° with respect to the direction expected for fully relaxed β-FeSi$_2$. We measured a smaller tilt angle of ~0.4° (Fig. 7), which indicates a partial relaxation of the strain in the film.

The measured blocking minimum is shallower than is expected for a fully relaxed β-FeSi$_2$ film of mixed 75% A/25% B orientation with bulk-like structure up to the very interface (dotted curve in Fig. 7). The difference must have its origin in lattice relaxations associated with the formation of atomic bonds across the interface. Although the data do not allow for a direct determination of the complex bonding arrangement at the interface, good agreement between measured and simulated Fe blocking patterns (solid curve, see also Fig. 5) is obtained for an interface model, which for the A orientation has the following structural features: (1) Two additional Si atoms at the silicide side of the interface so as to make the Fe atoms eightfold coordinated, (2) displacements of the interfacial Fe and Si atoms to positions halfway between those in the substrate and in the silicide lattice. Such an arrangement leaves no dangling bonds across the interface and leads to reasonable bond lengths for atom displacements as small as 0.8 Å. On the other hand, for the B orientation we cannot form such bonds without displacing the atoms over large distances or substantially changing in the bonding topology. For lack of a physically reasonable model for the B interface, we assumed in the simulations of the Fe blocking pattern a bulk-like bonding arrangement at the interface of B-oriented domains.

IV. DISCUSSION AND CONCLUSION

A silicide forming reaction is commonly observed if a transition metal is deposited at room temperature on an atomically clean surface.[22-24] The present study unambiguously establishes the formation of a FeSi film upon deposition of ~5 ML of Fe. We note that after deposition of similar quantities of Co or Ni, films of predominantly Ni$_2$Si and Co$_2$Si stoichiometry are formed.[23,24] In all three cases, the nucleated composition is close to the central eutectic in the metal-Si binary phase diagram, in line with the predictions of Ronay.[25] However, the nature of the silicides formed at lower coverages (between zero and two monolayers) has been a point of considerable debate.[26] For Ni and Co deposition, the formation of ultrathin precursor films of NiSi$_2$ and CoSi$_2$-like structures have been reported.[27,28] The possibility that a similar FeSi$_2$ precursor phase is formed for coverages below 2 ML will be discussed elsewhere.[29]

Our finding that a continuous FeSi film is formed disagrees with previous Auger and photoelectron spectroscopy (AES) studies, which reported the growth at RT of pure Fe films (islanded[4] or continuous[30]) with some Si mixed in. The origin of the disagreement is not clear.

For the (111) face, the formation at room temperature of pure epitaxial Fe films on Si was reported recently by Cheng et al.[31] Our study indicates that most likely also for this system some initial iron-silicide formation must have taken place.

Recently Geib et al.[6] have grown β-FeSi$_2$ films of pure B orientation by co-depositing Fe and Si in the stoichiometric ratio 1:2 at RT and subsequently annealing the film at low temperature (~550 K). They observed conversion into the more stable A orientation after heating above 650

K. Pure B films cannot be grown by the method employed here, i.e., by deposition of pure Fe at RT followed by heating; we obtain predominantly A-oriented films regardless of the heating temperature. One may wonder why the B orientation is formed at all, given the poor match with the substrate[6] and the substantial atomic rearrangements needed to eliminate the interfacial dangling bonds. For now, one can only speculate about the kinetic processes at work. Recently, we obtained β-FeSi$_2$ films of epitaxially pure A orientation by sequential deposition of 9 ML of Si and 5 ML of Fe at RT followed by heating.[31]

ACKNOWLEDGMENTS

[1] M. C. Bost and J. E. Mahan, J. Appl. Phys. **58**, 2696 (1985).

[2] P. Y. Dusausoy, J. Protas, R. Wandji, and B. Roques, Acta Cryst. B **27**, 1209 (1971).

[3] J. E. Mahan, K. M. Geib, G. Y. Robinson, R. G. Long, Y. Xinghua, G. Bai, M.-A. Nicolet, and M. Nathan, Appl. Phys. Let. **56**, 2126 (1990).

[4] S. Kennou, N. Cherief, R. C. Cinti, and T. A. Nguyen Tan, Surf. Sci. **211/212**, 685 (1989).

[5] J. Alvarez, J. J. Hinarejos, E. G. Michel, J. M. Gallego, A. L. Vazquez de Parga, J. de la Figuera, C. Ocal, and R. Miranda, Appl. Phys. Lett. **59**, 99 (1991).

[6] K. M. Geib, J. E. Mahan, R. G. Long, M. Nathan, and G. Bai, J. Appl. Phys. **70**, 1730 (1991).

[7] R. T. Tung and F. Schrey, Appl. Phys. Lett. **54**, 852 (1989).

[8] H. C. Cheng, T. R. Yew, and L. J. Chen, J. Appl. Phys. **57**, 5246 (1985).

[9] P. M. J. Marée, A. P. de Jong, J. W. Derks, and J. F. van der Veen, Nucl. Instrum. Methods B **28**, 76 (1987).

[10] J. F. van der Veen, Surf. Sci. Rep. **5**, 199 (1985).

[11] J. Vrijmoeth, P. M. Zagwijn, J. W. M. Frenken, and J. F. van der Veen, Phys. Rev. Lett. **67**, 1134 (1991).

[12] H. H. Andersen and J. F. Ziegler, *The Stopping and Ranges of Ions in Matter* (Pergamon, New York, 1977).

[13] W. K. Chu, J. W. Mayer, and M. A. Nicolet, *Backscattering Spectroscopy* (Academic, New York, 1978), Chap. II.

[14] R. M. Tromp and J. F. van der Veen, Surf. Sci. **133**, 159 (1983).

[15] J. Vrijmoeth, A. G. Schins, and J. F. van der Veen, Phys. Rev. B **40**, 3121 (1989).

[16] E. J. van Loenen, A. E. M. J. Fischer, F. LeGoues, and J. F. van der Veen, Surf. Sci. **154**, 52 (1985).

[17] R. M. Tromp, J. Vac. Sci. Technol. A **1**, 1047 (1983).

[18] R. M. Tromp, R. G. Smeenk, F. W. Saris, and D. J. Chadi, Surf. Sci. **133**, 137 (1983).

[19] M. Abramowitz and I. A. Stegun, *Handbook of Mathematical Functions* (Dover, London, 1965).

[20] H. Cheng, L. J. Chen, and T. R. Your, Mater. Res. Soc. Symp. Proc. **25**, 441 (1984).

[21] E. Vlieg, A. E. M. J. Fischer, J. F. van der Veen, B. N. Dev, and G. Materlik, Surf. Sci. **178**, 36 (1986).

[22] K. Okuno, T. Ito, M. Iwami, and A. Hiraki, Solid State Commun. **34**, 493 (1980).

[23] E. J. van Loenen, J. W. M. Frenken, and J. F. van der Veen, Appl. Phys. Lett. **45**, 1 (1984).

[24] J. F. van der Veen, A. E. M. J. Fischer, and J. Vrijmoeth, Appl. Surf. Sci. **38**, 13 (1989).

[25] M. Ronay, Appl. Phys. Lett. **42**, 577 (1983).

[26] P. J. Grunthaner, F. J. Grunthaner, and J. W. Mayer, J. Vac. Sci. Technol. **17**, 924 (1980).

[27] F. Comin, J. E. Rowe, and P. H. Citrin, Phys. Rev. Lett. **51**, 2402 (1983).

[28] J. Y. Veuillen, J. Derrien, P. A. Badoz, E. Rosencher, and C. d'Anterroches, Appl. Phys. Lett. **51**, 1448 (1987).

[29] K. Konuma, P. M. Zagwijn, E. Vlieg, and J. F. van der Veen (unpublished).

[30] J. M. Gallego, J. Alvarez, J. J. Hinarejos, E. G. Michel, and R. Miranda, Surf. Sci. **251/252**, 59 (1991).

[31] Y.-T. Cheng, Y.-L. Chen, M. M. Karmarka, and W.-J. Meng, Appl. Phys. Lett. **59**, 953 (1991).

[32] K. Konuma, P. M. Zagwijn, E. Vlieg, and J. F. van der Veen (unpublished).